

Strongly coupled gauge theories: What can lattice calculations teach us?

A. Hasenfratz*

*Department of Physics, University of Colorado,
Boulder, CO 80309, USA*

**E-mail: Anna.Hasenfratz@colorado.edu*

R.C. Brower, C. Rebbi and E. Weinberg

*Department of Physics and Center for Computational Science, Boston University,
Boston, MA 02215, USA*

O. Witzel

*Higgs Centre for Theoretical Physics, School of Physics & Astronomy,
The University of Edinburgh, Edinburgh, EH9 3FD, UK*

The dynamical origin of electroweak symmetry breaking is an open question with many possible theoretical explanations. Strongly coupled systems predicting the Higgs boson as a bound state of a new gauge-fermion interaction form one class of candidate models. Due to increased statistics, LHC run II will further constrain the phenomenologically viable models in the near future. In the meanwhile it is important to understand the general properties and specific features of the different competing models.

In this work we discuss many-flavor gauge-fermion systems that contain both massless (light) and massive fermions. The former provide Goldstone bosons and trigger electroweak symmetry breaking, while the latter indirectly influence the infrared dynamics. Numerical results reveal that such systems can exhibit a light 0^{++} isosinglet scalar, well separated from the rest of the spectrum. Further, when we set the scale via the v_{ev} of electroweak symmetry breaking, we predict a 2 TeV vector resonance which could be a generic feature of SU(3) gauge theories.

Keywords: composite Higgs, 2 TeV resonance, lattice field theory, 4+8 fundamental flavors, SU(3) gauge theory

1. Introduction

The Standard Model is a very successful description of electromagnetic, weak and strong interactions, yet the dynamical nature of its central feature, electroweak symmetry breaking (EWSB), has remained elusive. While experimental data strongly constrains physics Beyond the Standard Model (BSM), many options are still viable. New LHC results, such as the recently published di-boson resonance around 2 TeV, hint at new interactions^{1,2}. Increased statistics of LHC run II might finally reveal the origin of the Higgs boson and give insight into BSM physics.

Strongly coupled gauge-fermion systems are among the major contenders to describe BSM dynamics. In these models a new strongly interacting sector gives rise to

a new set of hadronic states that lead to experimentally verifiable predictions. While weakly coupled “QCD-like” systems are not compatible with electroweak precision measurements, recent non-perturbative lattice calculations show that strongly coupled systems, especially those near the conformal window, have properties that are very different from the weakly coupled models, making them good BSM candidates. There are several promising systems with different gauge and fermion content that have received significant attention lately, see e.g. [3-8](#). In this paper we describe a simple model that, while maybe not phenomenologically viable, can serve as basis of future, more sophisticated, and phenomenologically better motivated investigations. Preliminary results of our study have been presented in [9,10](#).

The strongly coupled BSM candidate models we are interested in must exhibit spontaneous chiral symmetry breaking. Their infrared (IR) spectrum contains three massless Goldstone pions and a relatively light 0^{++} scalar, in addition to a tower of additional massive states. When coupled to the electroweak sector the Goldstone pions become the longitudinal components of the W and Z bosons, triggering electroweak symmetry breaking. In this scenario the pseudoscalar (pion) decay constant F_π sets the scale of the BSM model, $F_\pi \approx 250$ GeV, the v_{ev} of EWSB. Among the massive states the 0^{++} meson plays the role of the Higgs boson, while the other states predicted by the model appear as heavy resonances at higher energies. Even though radiative corrections can significantly alter the mass of the 0^{++} scalar, for phenomenological applications it is desirable to have the isosinglet scalar well separated from the higher excitations.

If the model has only two massless fermions, there are only three Goldstone pions in the IR. However many models rely on more fermion flavors to push the system closer to the conformal window where non-perturbative effects can change the IR dynamics. In this case the IR spectrum contains many more Goldstone pion states than are required for EWSB. Those massless states have to acquire mass via a sequence of symmetry breaking steps between the UV and IR energy regions. While the explicit mechanism is model dependent and can be complicated, we can approximate the steps by lifting the mass of all but two fermions with explicit mass terms allowing them to decouple in the IR limit.

Theories that are either chirally broken or conformal but close to the conformal window can look very similar in a finite volume lattice study. Nevertheless, it is essential to ensure that the BSM candidate model breaks chiral symmetry spontaneously. If a gauge-fermion system turns out to be conformal, it has to be driven below the conformal window. This can easily be done by lifting the fermion masses in many-fermion systems as we do in this work. Alternatively, other interactions, possibly 4-fermion terms, may be added to ensure spontaneous chiral symmetry breaking.

2. The 4+8 flavor model

The model we consider in this work is based on the $SU(3)$ gauge theory with $N_f = 12$ fundamental flavors. This system is conformal when all 12 flavors are massless^{11–15}. Ideally we would like to lift the mass of 10 of the flavors to end up with a system that contains only 3 Goldstone pions in the IR. In this pilot study, however, we give mass only to 8 fermion species, keeping 4 in the chiral limit. The reason for this choice is technical. We use staggered fermions that naturally come in multiplets of four. It is possible to split the masses of the multiplets by taking the fourth root of the fermion determinant but taking the continuum limit requires special care, especially in strongly coupled systems. To avoid any potentially uncontrolled lattice artifacts we decided to consider a system with 4 massless (or at least light) and 8 heavy flavors.

Even if we kept only two fermions light, the $N_f = 12$ model is not ideal as it has a relatively small mass anomalous dimension. As we will argue in the next section, the anomalous dimension dictates scaling in the mass-split system as well. Systems closer to the conformal boundary, like $N_f = 10$ or perhaps 8 flavors could lead to phenomenologically more interesting systems. We are considering to investigate systems with 2+6 or 2+8 flavors in the future.

3. Wilson renormalization group description

The Wilson renormalization group (RG) approach applied for conformal and mass deformed conformal systems predicts the general scaling behavior of all dimensional quantities. In the following brief review we follow the notation of Ref.¹⁶, but extend that approach by allowing only a subset of the fermions to become massive while keeping the rest in the massless chiral limit.

Consider a 4-dimensional gauge-fermion system characterized by a set of gauge couplings g_i and masses m_i . Perturbatively, the gauge couplings are dimensionless while the dimension of the fermion mass is carried by the lattice cutoff. For convenience we introduce

$$\hat{m}_i = am_i \propto m_i/\Lambda_a, \quad (1)$$

with \hat{m}_i the dimensionless “lattice mass” and $\Lambda_a = \pi/a$ the lattice cutoff.

At the perturbative UVFP one of the gauge couplings, g_1 , is marginally relevant (the usual asymptotically free gauge coupling), while all other gauge couplings are irrelevant. The \hat{m}_i mass couplings are relevant at the perturbative UVFP and we assume they will stay relevant everywhere in the parameter space considered.

We choose the number of flavors such that the system is still asymptotically free but inside the conformal window, i.e. it has an IRFP at $(g_i = g_i^*, \hat{m}_i = 0)$ where all of the gauge couplings are irrelevant. If we tune the system to the conformal FP, it will be conformal at any energy range. Away but still close to the IRFP in the gauge couplings, at $(g_i \approx g_i^*, \hat{m}_i = 0)$, there are corrections to conformal behavior.

In the IR those die out and the system is conformal everywhere. Finite mass breaks conformality. If $\widehat{m}_i \gtrsim 0$ we have a mass-deformed system.

For the remainder of this section we will assume that the system is in the vicinity of the IRFP, i.e. the bare parameters as defined at the cutoff scale Λ_a are ($g_i \approx g_i^*$, $\widehat{m}_i \gtrsim 0$) and we can use Wilsonian RG equations to describe the parameter and energy scale dependence of any 2-point correlation function

$$C_H(t; g_i, \widehat{m}_i, \mu = \Lambda_a) = \int d^3x \langle H(t, x) H(0)^\dagger \rangle \Big|_{g, \widehat{m}, \Lambda_a}. \quad (2)$$

In the vicinity of the IRFP an RG transformation that changes the scale

$$\mu \rightarrow \mu' = \mu/b, \quad b > 1 \quad (3)$$

transforms the parameters as

$$\begin{aligned} (g_i(\mu) - g_i^*) &\rightarrow (g_i(\mu') - g_i^*) = b^{y_{g_i}} (g_i(\mu) - g_i^*), \\ \widehat{m}_i(\mu) &\rightarrow \widehat{m}_i(\mu') = b^{y_{m_i}} \widehat{m}_i(\mu) \end{aligned} \quad (4)$$

while the correlation function changes as

$$C_H(t; g_i, \widehat{m}_i, \mu) = b^{-2\gamma_H} C_H(t; g'_i, \widehat{m}'_i, \mu'). \quad (5)$$

Here γ_i denotes the anomalous dimension while $y_i = d_i + \gamma_i$ is the scaling dimension of the corresponding operator at the IRFP. Finally we rescale all dimensional quantities in Eq. (5) by b and obtain

$$C_H(t; g_i, \widehat{m}_i, \mu) = b^{-2y_H} C_H(t/b; g'_i, \widehat{m}'_i, \mu), \quad (6)$$

where for simplicity we do not indicate the explicit μ dependence of the couplings.

For the irrelevant couplings the scaling dimensions $y_i < 0$, while for relevant couplings $y_i > 0$. With repeated RG steps b increases and the irrelevant couplings g_i approach g_i^* . The fermion mass parameters, on the other hand, increase as $\widehat{m}_i \rightarrow b^{y_{m_i}} \widehat{m}_i$. The fermions decouple from the IR dynamics when $\widehat{m}'_i = \mathcal{O}(1)$ because the masses are now above the cutoff. For concreteness we choose $b = \widehat{m}_i^{-1/y_m}$, so $\widehat{m}(b^{y_m} \mu) = 1$ is the scale where the massive fermions no longer affect the IR dynamics.

It is worth noting that we can define b uniquely only if all massive fermions start with the same bare mass, $\widehat{m}_i(\Lambda_a) = \widehat{m}$. The RG equations become considerably more complicated if the fermions have different bare mass values. There is no complication however if we keep some fermions massless. These fermions will remain massless and present in the IR theory.

If b is large enough we can neglect any dependence on $g' - g_*$ and the RG equation of Eq. (6) reduces to

$$C_H(t; \widehat{m}_i(\mu), \mu) = \mathcal{C}_H F(t(\widehat{m})^{1/y_m}, \mu), \quad (7)$$

where F is some function that, for fixed μ , depends only on the rescaled variable $t(\widehat{m})^{1/y_m}$. Any 2-point correlation function is expected to show exponential behavior at large distances,

$$C_H(t; \widehat{m}_i, \mu) \propto e^{-M_H t}, \quad t \rightarrow \infty. \quad (8)$$

Combining equations (7) and (8) leads to the well-known (hyper)scaling relation

$$aM_H \propto (\widehat{m})^{1/y_m}. \quad (9)$$

If all fermions are massive, Eqs. (7) and (9) describe the scaling behavior of correlation functions of degenerate fermions. Equations (7) and (9) also describe correlation functions of pure gauge quantities and the scaling of glueballs, the square root of the string tension, etc. In the deep infrared limit the system is an $SU(N_c)$ gauge theory, no dynamical fermions are present. However this system is not identical to what we usually refer to as pure-gauge or quenched $SU(N_c)$ theory. The fermions, while decoupled in the IR, do influence the IR dynamics. As long as the system evolves from the scaling regime of the IRFP, the scaling relations of Eq. (9) hold for any bound states. The dimensionless ratios of physical quantities are expected to be independent of \widehat{m} , up to corrections to scaling due to both the irrelevant and relevant couplings.

The situation becomes more complicated if we keep some of the fermions massless, i.e. we have N_l flavors in the $\widehat{m}_\ell = 0$ chiral limit, while we give mass to N_h fermion flavors, $\widehat{m}_h > 0$. Equations (7) and (9) are still valid, but the correlation function $C_H(t)$ can contain operators constructed from massless fermions, massive fermions, or a combination of both. If the number of massless fermions, N_ℓ , is below the conformal window, the system is chirally broken and contains $N_\ell^2 - 1$ massless Goldstone pions in the IR. It also contains light hadronic states, similar to an N_l flavor $SU(N_c)$ theory in the chiral limit. States that contain at least one heavy flavor decouple and are not present in the deep IR limit, nevertheless their influence on the light hadron spectrum remains. All massive states, even those that contain only massless fermions, show hyperscaling with respect to the heavy flavor mass \widehat{m}_h . In particular, ratios of masses are expected to be independent of m_h (up to corrections due to scaling violations). While these ratios are governed by the conformal IRFP, their value can depend on N_ℓ , in addition to $N_\ell + N_h$ that determines the scaling dimensions at the IRFP.

3.1. The running gauge coupling

We consider first the running coupling of conformal and mass-deformed systems based on the Wilsonian RG discussion of the preceding section.

a) Conformal systems The solid curve in Fig. 1 depicts the running gauge coupling of a conformal system. All fermion masses are $\widehat{m}_i = 0$ and the quantity $\Lambda_a = \pi/a$ denotes the lattice scale where the bare parameter g_0 is set. If we want to

define a continuum theory at the perturbative UVFP the bare gauge coupling $g(\Lambda_a)$ has to be tuned to $g(\Lambda_a) \rightarrow 0$. As we lower the energy scale from Λ_a towards the IR, the gauge coupling changes according to Eq. (4), i.e. it approaches the IRFP. We denote the scale where the gauge coupling gets close enough to the IRFP such that $g(\mu) - g^*$ can be neglected by Λ_U , the UV scale where the dynamics governed by the IRFP sets in. The running gauge coupling at this scale takes the value of the IRFP, $g(\mu) \approx g^*$ and approaches g^* as $\mu \rightarrow 0$.

b) Mass deformed system Next we consider the case where all fermions acquire a small bare mass at the cutoff scale Λ_a . The running of the gauge coupling is only minimally affected until $\widehat{m}_i(\mu) = \mathcal{O}(1)$. We denote the scale where $\widehat{m}_i(\mu) = 1$ as Λ_{IR} , the IR scale where the fermions decouple. As the system runs deeper in the IR, the gauge coupling follows the running coupling of a pure gauge system. This behavior is denoted by the blue dashed curve in Fig. 1. Unless the bare fermion mass is tuned $\widehat{m}(\Lambda_a) \rightarrow 0$, in the deep IR a mass deformed system has only gauge degrees of freedom. That does not mean, however, that the system is equivalent to a pure gauge system, as we have discussed already in section 3.

c) Mass deformed systems far from the IRFP If the fermion mass at the cutoff level is too large, it is possible that $\Lambda_{IR} > \Lambda_U$. In that case the fermions decouple before the gauge coupling reaches the IRFP. This scenario is depicted by the red long-dashed lines in Fig. 1. In this case the IR dynamics is close to the pure gauge system with heavy fermions, and is not of interest for us.

d) Mass deformed system with split fermion masses In our final case we keep N_ℓ fermions massless and assign finite, degenerate bare mass $\widehat{m}(\Lambda_a)$ to the others. We will assume that $\widehat{m}(\Lambda_a)$ is small enough that $\Lambda_{IR} \ll \Lambda_U$ and that in the deep IR, where only the N_ℓ massless fermions contribute to the dynamics the system is chirally broken, i.e. N_ℓ is below the conformal window. Qualitatively the running coupling is very similar to that of the mass deformed system as discussed in case b). While the non-zero fermion masses are small the gauge coupling behaves like in a conformal system. At the Λ_{IR} scale the massive fermions decouple, chiral symmetry breaks and the IR system has N_ℓ massless fermions. The running gauge coupling is driven by this dynamics, similarly to the dashed blue line in Fig. 1. Just like in case b) this does not mean that the deep IR dynamics is equivalent to an $SU(N_c)$ gauge system with N_ℓ massless fermions. Before decoupling, the additional fermions have influenced the IR dynamics, leading to specific hyper scaling relations as we discussed in section 3.

3.2. The running coupling of the 4+8 flavor system

The gradient flow (GF) transformation provides a natural definition of the running coupling that is easy to implement numerically^{17–19}. The GF running coupling at

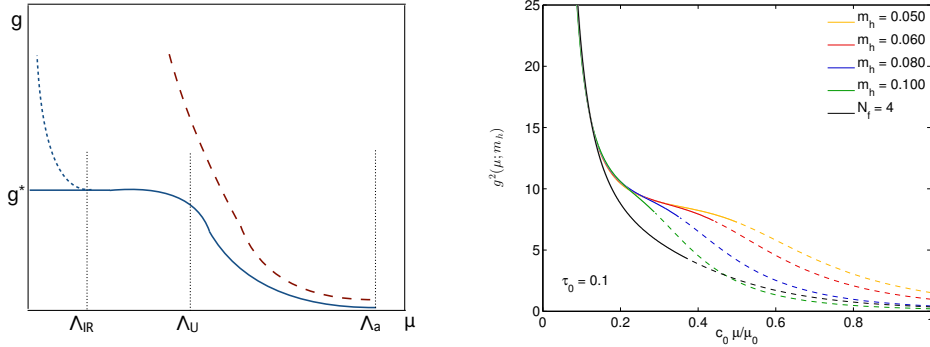


Fig. 1. Left: The expected running gauge coupling of conformal and mass-deformed system. The solid blue curve sketches the evolution of the gauge coupling with the energy scale in a conformal system. The dashed blue curve shows the modification in a mass deformed system while the red long-dashed curve corresponds to a situation where the fermions decouple before the gauge coupling could approach the conformal IRFP. Right: The running coupling constant \tilde{g}_{GF}^2 at the mass scale μ for different values of m_h with m_ℓ extrapolated to the chiral limit. μ_0 and $c_0 = \mu_0^{-1}|_{m_h=0.050}$ serve as normalization constants that ensure that the different systems are compared at matching energy scales and τ_0 is the shift parameter to remove discretization errors. The dashed sections of the lines indicate where we suspect cutoff effects may be significant. The running gauge coupling in our model at four different m_h mass values and in the $m_h = \infty$ 4-flavor limit. The emergence of the walking regime is evident as $m_h \rightarrow 0$.

energy scale μ is defined as

$$g_{GF}^2(\mu) = \frac{1}{\mathcal{N}} \langle t^2 E(t) \rangle, \quad (10)$$

where $t = a^2 t_{\text{lat}}$ ($t_{\text{lat}} \gg 1$) is the flow time that is related to the energy scale as $\mu^{-1} = \sqrt{8t}$. The energy density

$$E(t) = -\frac{1}{2} \text{ReTr}[G_{\mu\nu}(t)G^{\mu\nu}(t)] \quad (11)$$

can be evaluated by any appropriate lattice operator while the constant $\mathcal{N} = 3(N^2 - 1)/128\pi^2$ is chosen such that g_{GF}^2 matches the traditional \overline{MS} coupling in perturbation theory¹⁹.

We show $g_{GF}^2(\mu)$ as function of the energy μ from our numerical simulation of the 4+8 flavor system in the right panel of Fig. 1. We consider four different values for the heavy flavors and extrapolate to the chiral limit in the light quark masses. The right plot in Fig. 1 also shows the running coupling of the 4-flavor ($m_h = \infty$) system. We rescale μ by the lattice scale $\mu_0^{-1} = \sqrt{8t_0}$ (see¹⁹) in each case such that the running couplings match in the IR. The dashed curves correspond to flow time where $\sqrt{8t} \leq 2.0$ and cutoff effects could be important. While the choice $\sqrt{8t} = 2.0$ to separate discretization effects from physical behavior is rather arbitrary, the trend as the mass of the 8 heavy flavors decrease from ∞ towards the chiral limit is clear. The resemblance between the RG inspired behavior depicted on the left panel and the numerically observed prediction of the right panel is striking though

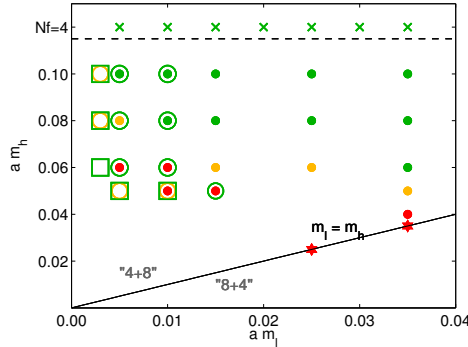


Fig. 2. Light (m_ℓ) and heavy (m_h) mass values for the simulations carried out on $24^3 \times 48$ lattices (filled symbols) and $32^3 \times 64$ lattice (open circles). The colors are meant to caution about finite size effects, likely negligible for green, but of increasing importance as the color turns to orange and red.

not unexpected: both show the theoretically well motivated running coupling of mass deformed systems near the conformal IRFP.

4. Numerical Simulations

Numerical simulations of our model with four light and eight heavy flavors are carried out using nHYP-smear²⁰ staggered fermions and the plaquette gauge action with fundamental and adjoint terms^{12,21}. In previous works^{12,21} with eight and twelve fundamental flavors, these actions demonstrated small taste breaking artifacts and with our choice of smearing parameters the numerical simulations are stable everywhere. We generated a large set of gauge field configurations with different bare input masses for the light and the heavy fermions at a single gauge coupling, $\beta = 4.0$. This gauge coupling is close enough to the $N_f = 12$ IRFP that the simulations can be considered to be in the mass deformed region. Starting with small volumes, $L^3 \times T = 24^3 \times 48$, we eventually increased the lattice sizes to $32^3 \times 64$, $36^3 \times 64$, and even $48^3 \times 96$ to study and account for finite volume effects. We present a graphical overview of our set of ensembles in Fig. 2 and indicate by the color the significance of finite volume effects: green (likely negligible), orange (moderate), red (severe). All gauge fields were generated by the hybrid Monte Carlo (HMC) update algorithm²² using the implementation in the FUEL software package²³.

As usual we monitor algorithmic parameters and physical observables during the evolution of gauge field configurations maintaining e.g. an average acceptance rate of greater 65% on all ensembles. Likewise we measure fermionic ($\langle \psi \bar{\psi} \rangle$) and gluonic (average plaquette) quantities and their dependence on the four space-time coordinates to detect artificial lattice phases. So far all our simulations are consistent with chiral symmetry breaking and do not exhibit any signs of the S4-broken lattice phase²⁴.

5. Spectrum

We have investigated the light fermion spectrum and the dependence of “hadronic” masses on the heavy input quark mass m_h . As we discussed in Sec. 3 we expect hyperscaling in the heavy mass m_h when the light mass m_ℓ is extrapolated to the chiral limit. Consequently dimensionless ratios should show independence on m_h up to lattice corrections.

In analogy to QCD we investigate “mesonic” quark-antiquark pairs, studying in particular the pseudoscalar (pion, π), vector (rho, ρ), axial-vector (a_1), and isotriplet scalar (a_0) bound states. Moreover, we determine the lowest mass baryon (three quark bound state), the nucleon (n). These quantities are described by quark-line connected diagrams, thus the numerical determination is straightforward and we obtain our results using propagators with wall-sources. In addition we determine the mass of the isosinglet scalar (0^{++}) meson bound state which has the same quantum numbers as the Higgs boson. Determining the isosinglet scalar is much more challenging because quark-line disconnected diagrams also contribute. These disconnected diagrams are numerically much noisier and require different numerical methods.

5.1. Connected light fermion spectrum

Using ensembles with sufficient number of thermalized trajectories and sufficiently large volumes, the left panel of Fig. 3 shows our results for the pion and the rho. We present the masses in units of a lattice reference scale a_\star which we define through the gradient flow $\sqrt{8t_0}$ scale on our $36^3 \times 64$, $m_h = 0.080$, $m_\ell = 0.003$ reference ensemble. Values in lattice units obtained on other ensembles are converted by multiplying appropriate ratios of the gradient flow scale^{17,19} which we determine on all ensembles.

As one expects based on the arguments in Sec. 3, the dependence on the input quark mass m_h is weak. Except for small finite volume effects, our measurements of the rho mass shows no dependence on m_h . The pion mass, M_π shows the same overall trend; however a small dependence on m_h , in particular for the heavier m_ℓ data sets is visible. Hyperscaling in m_h is only expected in the $m_\ell = 0$ limit. Our data are consistent with this expectation.

In the right panel of Fig. 3 we show the ratio M_ρ/M_π as function of the light quark mass. In contrast to a mass deformed conformal system (e.g. 12 flavors¹²), where all hadrons scale the same way with respect to the mass, we observe that for all our choices of m_h the ratio M_ρ/M_π is consistent with a divergent behavior for $m_\ell \rightarrow 0$. We take this as a certain indicator that in our simulations chiral symmetry is broken spontaneously in the limit of vanishing light quark mass.

In addition to the hadronic masses we also determine the pseudoscalar decay constant F_π which is the preferred choice for setting the scale in relation to EWSB. The quantity $F_\pi L$ controlling the chiral perturbative expansion is $1.0 \lesssim F_\pi L \lesssim 1.35$ for all our relevant data sets. However the smallness of this parameter is not the only

10

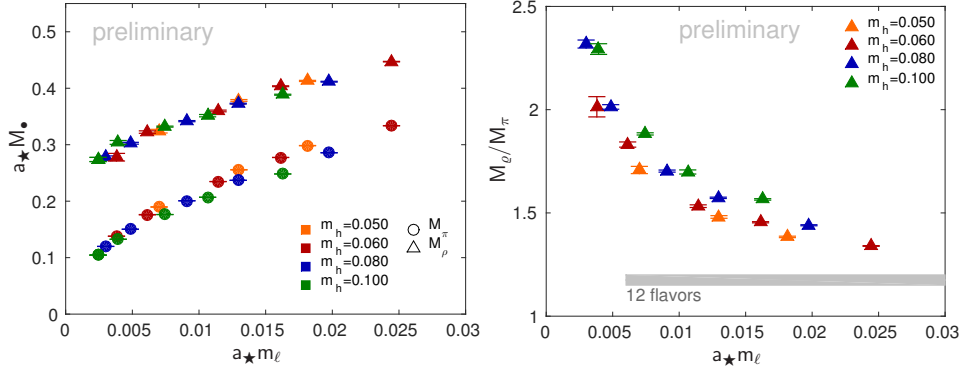


Fig. 3. Left: Pion and rho vs. light input quark mass shown in lattice units a_* defined on our $36^3 \times 64$, $m_h = 0.080$, $m_l = 0.003$ reference ensemble. The rho shows (except for small finite volume effects) no dependence on m_h and the pion exhibits only a very weak dependence, most pronounced at larger m_l values. Right: plotting the ratio M_ρ/M_π vs. the light input quark mass confirms that for $m_l \rightarrow 0$ chiral symmetry is broken for all our choices of m_h . As reference the value of M_ρ/M_π found in the corresponding 12 flavor system¹² is indicated by the grey band.

problem in performing a chiral extrapolation. The 0^{++} state, as will be discussed in the next section, is nearly degenerate with the pion, rendering standard chiral perturbative expansions and consequently chiral extrapolations questionable.

5.2. Determination of the isosinglet 0^{++} scalar

The determination of the isosinglet 0^{++} meson is more complicated and requires the evaluation of disconnected diagrams. We construct the disconnected operator from the vacuum subtracted operator

$$\mathcal{O}_{\text{disc}} = \langle \bar{\psi}\psi \rangle(t) - \langle \langle \bar{\psi}\psi \rangle \rangle_e, \quad (12)$$

and determine the vacuum contribution via the ensemble average $\langle \langle \bar{\psi}\psi \rangle \rangle_e$. The operator $\langle \bar{\psi}\psi \rangle(t)$ is measured using $N_r = 6$ full volume noise sources diluted in time, color, as well as spatially even/odd in order to reduce the stochastic noise.²⁵

In systems with degenerate flavors the 0^{++} state is the ground state of the correlator $ND(t) - C(t)$ where $D(t)$ and $C(t)$ are the disconnected and connected correlators of the scalar operator $\langle \bar{\psi}\psi \rangle(t) \langle \bar{\psi}\psi \rangle(0)$ and N denotes the number of flavors. When using staggered fermions $N = N_f/4$. In our case the physical 0^{++} correlator is more complicated as it is a mixture of light-light, light-heavy, and heavy-heavy scalar states. In addition the connected correlator couples strongly to excited states, making the determination of the 0^{++} numerically challenging. However, as was pointed out in Ref.²⁶, the ground state mass can be determined from the disconnected correlator alone. $D(t)$ couples to the 0^{++} state, and since that state is the lightest, it dominates the asymptotic behavior. Using only the disconnected correlator provides a numerically more stable determination of the lowest isosinglet scalar mass and avoids the cumbersome mixing of the light and

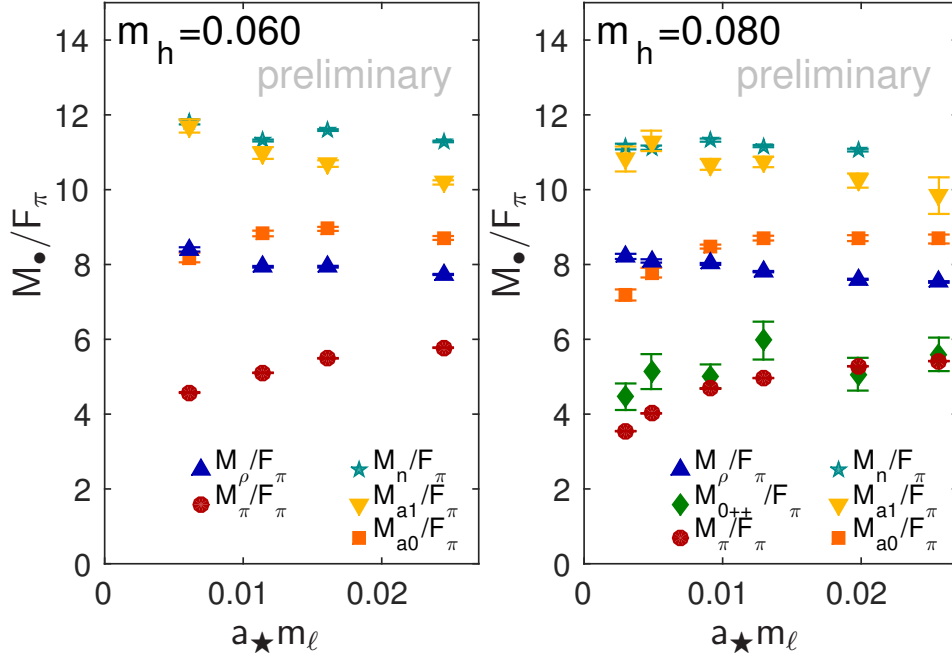


Fig. 4. Pion, rho, scalar 0^{++} , axial, a_0 , and nucleon mass of the light flavor spectrum in units of F_π as function of the light quark mass $a \star m_\ell$ for $m_h = 0.060$ and 0.080 . If a chirally broken system triggered EWSB, $F_\pi \approx 250$ GeV would set the correct electroweak scale.

heavy states as well. The vacuum subtraction in Eq. (12) is the source of large statistical fluctuations. In practice we find it is better to fit the finite difference $D(t+1) - D(t)$ of the disconnected correlator and avoid the vacuum subtraction altogether.

We perform measurements every 20 MDTU and have extended almost all of our Monte Carlo evolutions to at least 20,000 MDTU, in some cases even twice as much. Nevertheless the determination of the mass from the correlators is particularly difficult for larger values of m_ℓ . We therefore restrict the presentation of our 0^{++} results to the subset of our ensembles with $m_h = 0.080$. We expect hyperscaling in the $m_\ell = 0$ chiral limit, therefore the 0^{++} mass at any fixed m_h is indicative of its value everywhere in the scaling region of m_h .

6. Summary

The right panel of Fig. 4 summarizes our results for the 0^{++} isosinglet and several other isomultiplet states, normalized by the pion decay constant F_π , as the function of the light fermion mass m_ℓ at $m_h = 0.080$. The left panel shows the isomultiplet states at $m_h = 0.060$ where our statistics is not yet sufficient to determine the mass of the 0^{++} scalar. Hyperscaling, as we argued in Sec. 3, implies that all dimensionless ratios are identical, up to lattice corrections, in the $m_\ell = 0$ chiral

limit. Comparing the two panels of Fig. 4 shows that this expectation is satisfied by our data for the connected spectrum. There is no reason to believe that the 0^{++} scalar state would be any different.

Unlike in QCD, we observe a 0^{++} state at $m_h = 0.080$ that is nearly degenerate with the pion and much lighter than the rho. We have not attempted any kind of chiral extrapolation — standard chiral perturbation theory is based on the pion being the only light particle in the spectrum which is clearly not true in our case. Moreover we observe that M_ρ/F_π , M_{a_1}/F_π , and M_ρ/F_π have a fairly linear dependence on m_ℓ . In particular the ratio M_ρ/F_π appears nearly independent of both m_ℓ and m_h with a value around 8. Coincidentally if $F_\pi \approx 250$ GeV, the mass of the vector resonance in our model is around 2 TeV, matching the recently reported signal by ATLAS and CMS collaborations^{1,2}. It is a curiosity to note that $M_\rho/F_\pi \approx 8$ appears to be a rather general feature of SU(3) gauge fermion systems: this ratio is 8.4 in QCD²⁷; approximately 8.0 in the conformal SU(3) $N_f = 12$ model^{28,29}; about 7.9 with 8 fundamental flavors^{30,31}; approximately 8 in $N_f = 2$ flavor SU(3) sextet model³². Various theoretical models and approaches also predict that this ratio is independent of the specifics of the IR dynamics, see for example Refs.^{33,34}.

While we expect the dimensionless ratios to be independent of m_h , these ratios can depend on the details of the system, like the IRFP of the underlying conformal massless model and the number of light vs. heavy flavors. Comparing different systems could reveal which, if any, of these models are potentially compatible with experimental observations.

Our work is just the first step in this direction. Choosing a system with two (or four) massless and many massive fermions ensure that in the IR the model is chirally broken while choosing the total number of fermions such that in the massless limit the system is conformal ensures hyper scaling. While a similar construction is possible even if the underlying mass-degenerate system is not conformal, it is not obvious what kind of scaling relations one can obtain in that case.

In the future we would like to extend these investigation to systems with 2 massless fermions with $N_f = N_\ell + N_h$ closer to the conformal window. Numerical simulations indicate that systems with $N_f = 8$ or 10 fundamental fermions exhibit large mass anomalous dimensions, making them better candidates to satisfy electroweak constraints.

Acknowledgments

Computations for this work were carried out in part on facilities of the USQCD Collaboration, which are funded by the Office of Science of the U.S. Department of Energy, on computers at the MGHPCC, in part funded by the National Science Foundation, and on computers allocated under the NSF Xsede program to the project TG-PHY120002. We thank Boston University, Fermilab, the NSF and the U.S. DOE for providing the facilities essential for the completion of this work. R.C.B., C.R. and E.W. were supported by DOE grant DE-SC0010025 and in ad-

dition acknowledge the support of NSF grant OCI-0749300. A.H. acknowledges support by the DOE grant DE-SC0010005. O.W. is supported by STFC, grant ST/L000458/1. R.C.B., A.H. and C.R. thank the Aspen Center for Physics, which is supported by National Science Foundation grant PHY-1066293. R.C.B., A.H., and O.W. thank the KITP, Santa Barbara, supported in part by the National Science Foundation under Grant No. NSF PHY11-25915.

References

1. ATLAS Collaboration, Search for high-mass diboson resonances with boson-tagged jets in proton-proton collisions at $\sqrt{s} = 8$ TeV with the ATLAS detector (2015).
2. CMS Collaboration, Search for massive WH resonances decaying to $\ell\nu b\bar{b}$ final state in the boosted regime at $\sqrt{s} = 8$ TeV (2015).
3. ATLAS Collaboration, Search for high-mass dilepton resonances in pp collisions at $\sqrt{s} = 8$ TeV with the ATLAS detector, *Phys. Rev.* **D90**, p. 052005 (2014).
4. A. Arbey, G. Cacciapaglia, H. Cai, A. Deandrea, S. Le Corre and F. Sannino, Fundamental Composite Electroweak Dynamics: Status at the LHC (2015).
5. Y. Aoki *et al.*, Light composite scalar in eight-flavor QCD on the lattice, *Phys.Rev.* **D89**, p. 111502 (2014).
6. A. Hietanen, R. Lewis, C. Pica and F. Sannino, Fundamental Composite Higgs Dynamics on the Lattice: SU(2) with Two Flavors, *JHEP* **07**, p. 116 (2014).
7. Z. Fodor, K. Holland, J. Kuti, S. Mondal, D. Nogradi and C. H. Wong, Toward the minimal realization of a light composite Higgs, *PoS LATTICE2014*, p. 244 (2015).
8. D. Schaich, A. Hasenfratz and E. Rinaldi, Finite-temperature study of eight-flavor SU(3) gauge theory (2015).
9. R. Brower, A. Hasenfratz, C. Rebbi, E. Weinberg and O. Witzel, A novel approach to the study of conformality in the SU(3) theory with multiple flavors, *J. Exp. Theor. Phys.* **120**, 423 (2015).
10. R. Brower, A. Hasenfratz, C. Rebbi, E. Weinberg and O. Witzel, Targeting the conformal window with 4+8 flavors, *PoS LATTICE2014*, p. 254 (2014).
11. A. Cheng, A. Hasenfratz, G. Petropoulos and D. Schaich, Scale-dependent mass anomalous dimension from Dirac eigenmodes, *JHEP* **1307**, p. 061 (2013).
12. A. Cheng, A. Hasenfratz, Y. Liu, G. Petropoulos and D. Schaich, Finite size scaling of conformal theories in the presence of a near-marginal operator, *Phys.Rev.* **D90**, p. 014509 (2014).
13. M. P. Lombardo, K. Miura, T. J. N. da Silva and E. Pallante, On the particle spectrum and the conformal window, *JHEP* **12**, p. 183 (2014).
14. E. Itou, The anomalous dimension at the infrared fixed point of Nf = 12 SU(3) theory, *PoS LATTICE2013*, p. 481 (2013).
15. E. Itou and A. Tomiya, Determination of the mass anomalous dimension for

- $N_f = 12$ and $N_f = 9$ SU(3) gauge theories, PoS LATTICE2014, p. 252 (2014).
16. L. Del Debbio and R. Zwicky, Hyperscaling relations in mass-deformed conformal gauge theories, Phys. Rev. **D82**, p. 014502 (2010).
 17. R. Narayanan and H. Neuberger, Infinite N phase transitions in continuum Wilson loop operators, JHEP **0603**, p. 064 (2006).
 18. M. Lüscher, Trivializing maps, the Wilson flow and the HMC algorithm, Commun.Math.Phys. **293**, 899 (2010).
 19. M. Lüscher, Properties and uses of the Wilson flow in lattice QCD, JHEP **1008**, p. 071 (2010).
 20. A. Hasenfratz, R. Hoffmann and S. Schaefer, Hypercubic smeared links for dynamical fermions, JHEP **0705**, p. 029 (2007).
 21. A. Cheng, A. Hasenfratz, G. Petropoulos and D. Schaich, Determining the mass anomalous dimension through the eigenmodes of Dirac operator, PoS LATTICE2013, p. 088 (2013).
 22. S. Duane, A. Kennedy, B. Pendleton and D. Roweth, Hybrid Monte Carlo, Phys.Lett. **B195**, 216 (1987).
 23. J. Osborn et al., Framework for unified evolution of lattices (FUEL).
 24. A. Cheng, A. Hasenfratz and D. Schaich, Novel phase in SU(3) lattice gauge theory with 12 light fermions, Phys.Rev. **D85**, p. 094509 (2012).
 25. J. Foley, K. Jimmy Juge, A. Ó Cais, M. Peardon, S. M. Ryan and J.-I. Skullerud, Practical all-to-all propagators for lattice QCD, Comput. Phys. Commun. **172**, 145 (2005).
 26. Y. Aoki et al., Light composite scalar in twelve-flavor QCD on the lattice, Phys.Rev.Lett. **111**, p. 162001 (2013).
 27. K. A. Olive et al., Review of Particle Physics, Chin. Phys. **C38**, p. 090001 (2014).
 28. Z. Fodor et al., Twelve massless flavors and three colors below the conformal window, Phys.Lett. **B703**, 348 (2011).
 29. Y. Aoki, T. Aoyama, M. Kurachi, T. Maskawa, K.-i. Nagai et al., Lattice study of conformality in twelve-flavor QCD, Phys.Rev. **D86**, p. 054506 (2012).
 30. Y. Aoki et al., Walking signals in $N_f = 8$ QCD on the lattice, Phys.Rev. **D87**, p. 094511 (2013).
 31. LSD collaboration, in preparation (2015).
 32. J. Kuti, The simplest composite higgs candidate with resonance spectrum in the 2-teV range talk at KITP, Santa Barbara “Lattice Gauge Theory for the LHC and Beyond” on Aug. 5, 2015.
 33. H. Pagels and S. Stokar, The Pion Decay Constant, Electromagnetic Form-Factor and Quark Electromagnetic Selfenergy in QCD, Phys. Rev. **D20**, p. 2947 (1979).
 34. T. Appelquist and L. C. R. Wijewardhana, Chiral Hierarchies and Chiral Perturbations in Technicolor, Phys. Rev. **D35**, p. 774 (1987).